Int. J. Electron. Commun. (AEÜ) xxx (2016) xxx–xxx

Contents lists available at ScienceDirect

International Journal of Electronics and Communications (AEÜ)

journal homepage: www.elsevier.com/locate/aeue

Regular Paper

Pilot distribution optimization in multi-cellular large scale MIMO systems

José Carlos Marinello, Taufik Abrão *

State University of Londrina, Electrical Engineering Department (DEEL-UEL), Rod. Celso Garcia Cid – PR445, s/n, Campus Universitário, Po. Box 10.011, 86057-970 Londrina, Parana, Brazil

ARTICLE INFO

Article history:
Received 11 February 2016
Accepted 11 May 2016
Available online xxxx

Keywords:
Massive MIMO systems
BER
Multiuser MIMO
Precoding
Pilot sequences

ABSTRACT

Salient characteristics of a wireless communication system deploying a great number of antennas at the base station (BS), namely a massive MIMO system, are investigated in this work. The asymptotic performance of the linear zero-forcing precoding scheme is found, both in terms of signal-to-interference-plus-noise ratio (SINR) and bit-error rate (BER), and shown to be equivalent to the matched-filter beamforming performance. Furthermore, analysis of the massive MIMO system downlink is carried out from the viewpoint of uncoded BER performance, including some realistic adverse effects, such as interference from neighbouring cells, channel estimation errors due to background thermal noise, and pilot contamination. The latter has been shown to be the only impairment that remains in the MIMO multicell system with infinite number of BS antennas. For such scenario, we derive expressions for the asymptotic BER, *i.e.* in the limit of infinite number of antennas at BS. A quite simple and efficient method for optimizing the massive MIMO system performance under different optimization metrics is proposed, which consists of simply distributing the pilot sequences among the users of the cell in an efficient manner. As a result, a user rate gain of six times regarding the random strategy has been achieved for the downlink with unitary reuse factor, while the user rate increases twice for reuse factor of three. These benefits are achieved by only knowing the powers and the long-term fading coefficients of users in adjacent cells, for each pilot sequence.

1. Introduction

Multiple-input–multiple-output (MIMO) techniques constitute one of the key features in most of recent telecommunications standards, such as WiFi, WiMAX, LTE [6]. In order to fully exploit the benefits of MIMO systems, a new concept has been proposed by increasing the number of base station (BS) antennas N to infinity [9]. This massive MIMO systems are viewed as a potential technology for physical layer in next telecommunications standards, such as 5G [2]. A review of most important results recently disseminated in this theme can be found in [17].

It was shown in [9] that in a time division duplex (TDD) noncooperative multi-cell MIMO system, employing training pilots for channel state information (CSI) acquisition in the uplink and an infinite number of BS antennas, the effects of uncorrelated thermal noise and fast fading are averaged out. Hence, the only factor that remains limiting performance in the large MIMO scenario is inter-cell interference, that when associated with the finite time available to send pilot sequences makes the estimated CSI at one BS "contaminated" by the CSI of users in adjacent cells, in the so-called pilot contamination effect. This phenomenon results from unavoidable reuse of reverse-link pilot sequences by terminals in different cells. As a consequence of increasing the number of BS antennas to infinity, the transmit power can be designed arbitrarily small, since interference decreases in the same rate of the desired signal power, *i.e.*, signal-to-interference-plus-noise ratio (SINR) is independent of transmit power [9].

Alternative strategies to achieve better CSI estimates exist, such as (a) frequency division duplex (FDD) [3], in which pilots for CSI acquisition are transmitted in downlink, and estimates are fed back to BS in a feedback channel; and (b) network MIMO [7], where CSI and information data of different coordinated cells are shared among them in a backhaul link, creating a distributed antenna array that serves the users altogether. However, both schemes become unfeasible when $N \to \infty$ [9], since lengths of forward pilot sequences and capacity of backhaul links increase substantially with N. Therefore, TDD has been assumed in this work without CSI sharing among different cells.

* Corresponding author. Tel.: +55 43 3371 4790.
E-mail addresses: zecarlos.ee@gmail.com (J.C. Marinello), taufik@uel.br (T. Abrão).

http://dx.doi.org/10.1016/j.aeue.2016.05.007
1434-8411/

Operating with a large excess of BS antennas compared with the number of terminals K is a challenging but desirable condition, since some results from random matrix theory become applicable [4]. It is known, for instance, that very tall/wide matrices tend to be very well conditioned, since their singular values distribution appears to be deterministic, showing a stable behavior (low variances) and a relatively narrow spread [14]. Besides, in the large scale MIMO, the most simple reception/transmission techniques, *i.e.*, maximum ratio combining (MRC) deployed in the uplink and the matched-filtering (MF) precoding used in the downlink, become optimal [14].

An interesting investigation about precoding techniques of single-cell multiuser MIMO systems downlink is carried out in [16]. Specifically, authors compared MF precoding, also known as conjugate beamforming, and zero-forcing (ZF) beamforming, with respect to net spectral-efficiency and radiated energy-efficiency in a simplified single-cell scenario. It is found that, for high spectral-efficiency and low energy-efficiency, ZF outperforms MF, while at low spectral-efficiency and high energy-efficiency the opposite holds. A similar result is found for the uplink in [11], where for low signal-to-noise ratio (SNR), the simple MRC receiver outperforms the ZF receiver. On the other hand, when considering the multi-cell environment, it is found in [14] that the asymptotic SINR of MF outperforms ZF, although MF requires much more antennas to approach the asymptotic condition.

A more rigorous expression for the achievable SINR of MF precoding in massive MIMO systems, in comparison with that derived in [9] and adopted in [14], has been obtained in [5]. Authors of latter showed that, for downlink, the effect of the transmit power constraint at BS still accounts in the massive MIMO regime, as opposed to what was assumed in [9]. Besides, authors of [5] discuss an efficient technique for temporally distribute the uplink transmissions of pilot sequences, avoiding simultaneous transmissions from adjacent cells and reducing interference as well, in conjunction with power allocation strategy. On the other hand, a precoding technique that eliminates pilot contamination and leads to unlimited gains with $N \to \infty$ has been proposed in [1]. However, these gains come at the expense of sharing the information data between BSs, what can overload the backhaul signaling channel for high rate systems, or high number of users per cell.

An analysis of *non-linear precoding* techniques applied to the downlink of a massive MIMO system is conducted in [10]. Authors investigated the time domain vector perturbation (TDVP) scheme, which has been shown previously to almost achieve the downlink capacity of conventional MIMO channels. However, in the large-system analysis, it was shown that linear precoding schemes outperforms TDVP, in terms of increased sum rates, regardless of the user scheduling method adopted. Thus, linear precoding techniques has been investigated in our contribution. In [18], the pilot contamination is tackled by dividing the users within each cell in two groups, which are: the center users, and the edge users. As the edge users would suffer from severe pilot contamination if the same set of pilot sequences were reused by every cell, it is assigned for each edge user an exclusive training sequence in a cluster of L cells, while the center users reuse the same pilot's set. Although this so-called soft pilot reuse scheme effectively reduces the pilot contamination, the cost of devoting orthogonal pilots for every edge user may limit its practical appeal in TDD systems. Hence, we aim to reduce the pilot contamination in this paper adopting the challenging but realistic scenario of full pilot reuse among cells.

In this paper, we focus on the pilot distribution optimization and its impact on the performance of multi-cellular massive MIMO systems. The novelty and contributions of this paper are as follows:

(i) We derive an analytical expression for the downlink SINR system under ZF precoding, considering the effect of power constraint at BS. It is shown that the achieved SINR corresponds to the same value achieved by MF, as opposed to what is found in [14] neglecting the effects of the transmit power constraint.

(ii) Different from previous works that have analysed the SINR and the capacity of the massive MIMO system [9,5,14], we investigate also its downlink uncoded bit-error rate (BER) performance, which is another important figure of merit in communication systems. An exact expression for the BER of each user is derived, depending on the transmit power of users and on the long-term fading coefficients.

(iii) We propose a novel and expedite method of optimizing the massive MIMO downlink transmission under different metrics, based on our derived BER expression, and on the asymptotic SINR expression of [5]. This method consists of simply assigning the available training sequences among the users within a cell in an efficient manner, by knowing only the power and the long-term fading coefficients of users in adjacent cells that reuse such pilot sequences. Different pilot allocation metrics enable us to minimize the average BER, or maximize the average SINR, minimize the maximal BER or even maximize the minimum SINR. The proposed algorithms can lead to appreciable performance gains, both in terms of data rate, as well as in terms of BER of a massive MIMO system.

The paper is organized as follows. Beyond this introductory Section, the system model is described in Section 2. Some asymptotic limits of the massive MIMO system are revisited and extended in Section 3. Our proposed methods of assigning the pilots among the users within the cell in an efficient manner, namely the Pilot Allocation (PA) schemes, are presented in Section 4. Representative numerical results are discussed in Section 5, while Section 6 concludes the paper.

1.1. Notations

Boldface lower and upper case symbols represent vectors and matrices, respectively. $\mathbf{I}_N$ denotes the identity matrix of size N, while $\mathbf{1}_K$ and $\mathbf{0}_K$ are the unitary vector and null vector of length K, respectively. The transpose and the Hermitian transpose operator are denoted by $\{\cdot\}^T$ and $\{\cdot\}^H$, respectively, while $\mathrm{diag}(\cdot)$ is the diagonal matrix operator. $\|\cdot\|$ is the Euclidean norm of a vector. We use $\mathcal{CN}(\mathbf{m},\mathbf{V})$ to refer to a circular symmetric complex Gaussian distribution with mean vector $\mathbf{m}$ and covariance matrix $\mathbf{V}$. Also, $\mathbb{E}[\cdot]$ denotes the expectation operator, $\mathrm{u}[x]$ is the Heaviside step function ($\mathrm{u}[x]=1$ if $x \geqslant 0, \mathrm{u}[x]=0$ otherwise), while δ_{ij} is the Kronecker delta function ($\delta_{ij}=1$ if $i=j$ and 0 otherwise).

2. System model

The adopted MIMO system is composed by L BSs, each equipped with N transmit antennas, reusing the same spectrum and the same set of K pilot signals. Since TDD is assumed, reciprocity holds, and thus CSI is acquired by means of uplink training sequences. During a channel coherence time interval, the symbol periods are divided in uplink pilot transmissions, processing, downlink and uplink data transmissions [5,18]. Using orthogonal pilot sequences, the number of available sequences is equal to its length, K. Thus, K is limited due to mobility of the users, which reduces the coherence time of the channel. Orthogonal frequency-division

Please cite this article in press as: Marinello JC, Abrão T. Pilot distribution optimization in multi-cellular large scale MIMO systems. Int J Electron Commun (AEÜ) (2016), http://dx.doi.org/10.1016/j.aeue.2016.05.007

multiplexing (OFDM) is assumed in the same way as in [9]. The channel coherence band is divided into N_{smooth} subcarriers, and each subcarrier is shared by K users. As discussed in [9], dividing the channel coherence band by the subcarrier spacing,

$$N_{\text{smooth}} = \frac{1-\Delta t_{CP}}{\Delta t_{CP}}, \tag{1}$$

where Δt_{CP} is the fraction of the OFDM symbol duration devoted to the cyclic prefix, typically about 7% in current standards. Note that only one out of N_{smooth} subcarriers is assigned to a certain user for each coherence band; therefore, a total number of $K \cdot N_{\text{smooth}}$ users is allowed for each cell. We assume perfect orthogonality in the frequency domain, such that interference is only due to the K users sharing the same subcarrier. Hence, we define our model for a generic subcarrier, assuming flat fading environment in which the BS communicates with K users equipped with single-antenna mobile terminals (MTs). We denote the $1 \times N$ channel vector between the ℓth BS and the kth user of jth cell by $\mathbf{g}_{\ell kj} = \sqrt{\beta_{\ell kj}}\mathbf{h}_{\ell kj}$, in which $\beta_{\ell kj}$ is the long-term fading power coefficient, that comprises path loss and log-normal shadowing, and $\mathbf{h}_{\ell kj}$ is the short-term fading channel vector, that follows $\mathbf{h}_{\ell kj} \sim \mathcal{CN}(\mathbf{0}_N, \mathbf{I}_N)$. The channel matrix $\mathbf{H}$ is admitted constant over the entire frame and changes independently from frame to frame (block fading channel assumption). Note that $\beta_{\ell kj}$ is assumed constant for all N BS antennas. For the kth user of each cell in a given subcarrier, it is assigned the sequence $\boldsymbol{\psi}_k = [\psi_{1k}\ \psi_{2k} \dots \psi_{Kk}]^T$, $\boldsymbol{\psi}_k \in \mathbb{C}^{K\times 1}$. It holds that $|\psi_{ik}| = 1$ and $|\boldsymbol{\psi}_k^H \boldsymbol{\psi}_{k'}| = K\delta_{kk'}$ since the set of sequences is orthogonal.

In the training transmission phase, we have assumed synchronization in the uplink pilot transmissions, since this situation characterizes the worst case for inter-cellular interference [9]. Hence, the $N \times K$ received signal at the ℓth BS is:

$$\mathbf{Y}_\ell = \sum_{j=1}^{L} \mathbf{G}_{\ell j}^T \sqrt{\boldsymbol{\Gamma}_j}\boldsymbol{\Psi} + \mathbf{N}, \tag{2}$$

where $\boldsymbol{\Gamma}_j = \text{diag}(\gamma_{1j}\ \gamma_{2j} \dots \gamma_{Kj})$, being γ_{kj} the uplink transmit power of the kth user of jth cell, $\mathbf{G}_{\ell j} = [\mathbf{g}_{\ell 1j}^T\ \mathbf{g}_{\ell 2j}^T \dots \mathbf{g}_{\ell Kj}^T]^T$, such that the $K \times N$ matrix $\mathbf{G}_{\ell j} = \sqrt{\mathcal{B}_{\ell j}}\mathbf{H}_{\ell j}, \mathcal{B}_{\ell j} = \text{diag}(\beta_{\ell 1j}\ \beta_{\ell 2j} \dots \beta_{\ell Kj}), \mathbf{H}_{\ell j} = [\mathbf{h}_{\ell 1j}^T\ \mathbf{h}_{\ell 2j}^T \dots \mathbf{h}_{\ell Kj}^T]^T$ is of dimension $K \times N$, $\boldsymbol{\Psi} = [\boldsymbol{\psi}_1\ \boldsymbol{\psi}_2 \dots \boldsymbol{\psi}_K]$, and $\mathbf{N}$ is a $N \times K$ additive white Gaussian noise (AWGN) matrix whose entries have zero mean and unitary variance.

In order to generate the estimated CSI matrix $\widehat{\mathbf{G}}_\ell$ of their served users, the ℓth BS correlates its received signal matrix with the known pilot sequences:

$$\widehat{\mathbf{G}}_\ell^T = \frac{1}{K}\mathbf{Y}_\ell \boldsymbol{\Psi}^H = \sum_{j=1}^{L} \mathbf{G}_{\ell j}^T \sqrt{\boldsymbol{\Gamma}_j} + \mathbf{N}', \tag{3}$$

where $\mathbf{N}' \in \mathbb{C}^{N\times K}$ is an equivalent AWGN matrix with zero mean and variance $\frac{1}{K}$. Hence, the channel estimated by the ℓth BS is contaminated by the channel of users that use the same pilot sequence in all other cells.

Information transmit symbols of the ℓth cell is denoted by the $K \times 1$ vector $\mathbf{x}_\ell = [x_{1\ell}\ x_{2\ell} \dots x_{K\ell}]^T$, where $x_{k\ell}$ is the transmit symbol to the kth user of the ℓth cell, and takes a value from the squared quadrature amplitude modulation (M-QAM) alphabet, normalized in order to preserve unitary average power. For analysis simplicity, using matrix notation, the $K \times 1$ complex-valued signal received by users of the ℓth cell is written as:

$$\mathbf{r}_\ell = \sum_{j=1}^{L} \mathbf{G}_{j\ell}\mathbf{P}_j \sqrt{\boldsymbol{\Phi}_j}\mathbf{x}_j + \mathbf{n}_\ell, \tag{4}$$

where $\boldsymbol{\Phi}_j = \text{diag}(\phi_{1j}\ \phi_{2j} \dots \phi_{Kj})$, being ϕ_{kj} the downlink transmit power devoted by the jth BS to its kth user, $\mathbf{P}_j$ denotes the complex valued $N \times K$ precoding matrix of the jth BS, being each column $\mathbf{p}_{kj}$ the $N \times 1$ precoding vector of the kth user. Finally, $\mathbf{n}_\ell \sim \mathcal{CN}(\mathbf{0}_K, \mathbf{I}_K)$ represents the AWGN vector observed at the K MTs of the ℓth cell.

Under the matched-filter beamforming technique, the vector $\mathbf{p}_{kj}$ is computed as [5]:

$$\mathbf{p}_{kj}^{mf} = \frac{\widehat{\mathbf{g}}_{jk}^H}{||\widehat{\mathbf{g}}_{jk}^H||} = \frac{\widehat{\mathbf{g}}_{jk}^H}{\alpha_{kj}\sqrt{N}}, \tag{5}$$

in which $\alpha_{kj} = \frac{||\widehat{\mathbf{g}}_{jk}^H||}{\sqrt{N}}$, and $\widehat{\mathbf{g}}_{jk}$ is the kth row of the matrix $\widehat{\mathbf{G}}_j$. Note that the normalization in (5) is necessary to satisfy the maximum transmit power available at the BS.

In the same way, in the zero-forcing beamforming technique, the vector $\mathbf{p}_{kj}$ is computed as:

$$\mathbf{p}_{kj}^{zf} = \frac{\mathbf{w}_{jk}}{||\mathbf{w}_{jk}||}, \tag{6}$$

in which the vector $\mathbf{w}_{jk} = \widehat{\mathbf{G}}_j^H \mathbf{a}_{jk}$, and $\mathbf{a}_{jk}$ is the kth column of $\mathbf{A}_j = \left[\widehat{\mathbf{G}}_j \widehat{\mathbf{G}}_j^H\right]^{-1}$.

3. Asymptotic limits of massive MIMO

Most of the asymptotic limits for massive MIMO systems can be build upon the following well known lemma:

Lemma 1. *Let $\mathbf{s}_1, \mathbf{s}_2 \in \mathbb{C}^{N\times 1}$ be two independent complex-valued vectors following a normal distribution, with zero mean and variance σ^2. Then*

$$\lim_{N\to\infty} \frac{\mathbf{s}_1^H \mathbf{s}_2}{N} \overset{a.s.}{=} 0 \quad \text{and} \quad \lim_{N\to\infty} \frac{\mathbf{s}_1^H \mathbf{s}_1}{N} \overset{a.s.}{=} \sigma^2. \tag{7}$$

Since the channel vectors of different users can be seen as independent random vectors, the above lemma is widely used for deriving limits in the massive MIMO scenarios. It can be justified since as the vector's length grows, the inner products between independent vectors grow at lesser rates than the inner products of vectors with themselves.

3.1. Asymptotic limits of MF beamforming

From (3), it is proved in [5] that $\alpha_{kj}^2 \overset{a.s.}{=} \sum_{l=1}^{L}\gamma_{kl}\beta_{jkl} + \frac{1}{K}$. Then authors show that $r_{k\ell}$, *i.e.*, the received signal at the kth user of ℓth cell, can be written as [5, Eq. (5)]:

$$r_{k\ell} = \sum_{l=1}^{L}\sum_{j=1}^{K} \sqrt{\phi_{jl}\beta_{lk\ell}}\mathbf{h}_{lk\ell}^H \mathbf{p}_{jl}^{\text{mf}} x_{jl} + n_{k\ell}. \tag{8}$$

Based on (5) and Lemma 1, (8) can be simplified when $N \to \infty$ as:

$$\begin{aligned} r_{k\ell} &= \sum_{l=1}^{L} \sqrt{\phi_{kl}\beta_{lk\ell}}\mathbf{h}_{lk\ell}^H \mathbf{p}_{kl}^{\text{mf}} x_{kl} + n_{k\ell}, \\ &= \sum_{l=1}^{L} \frac{1}{\alpha_{kl}} \sqrt{N\phi_{kl}\gamma_{k\ell}}\beta_{lk\ell} x_{kl} + n_{k\ell}, \\ &= \sqrt{N\gamma_{k\ell}} \sum_{l=1}^{L} \frac{\sqrt{\phi_{kl}}\beta_{lk\ell}x_{kl}}{\alpha_{kl}} + n_{k\ell}. \end{aligned} \tag{9}$$

Note that the AWGN of the estimated CSI in (3) vanishes in (9). This occurs since it is independent of $\mathbf{h}_{lk\ell}^H$, and thus its product as $N \to \infty$ is averaged out according to Lemma 1.

From (9), it is straightforward to see the asymptotic downlink SINR of the system as:

Please cite this article in press as: Marinello JC, Abrão T. Pilot distribution optimization in multi-cellular large scale MIMO systems. Int J Electron Commun (AEÜ) (2016), http://dx.doi.org/10.1016/j.aeue.2016.05.007

$$\mathrm{SINR}_{k\ell}^{dl} = \lim_{N\to\infty} \frac{N\gamma_{k\ell}\,\phi_{k\ell}\beta_{\ell k\ell}^2/\alpha_{k\ell}^2}{N\gamma_{k\ell}\left(\sum_{\substack{j=1\\ j\neq\ell}}^{L}\phi_{kj}\beta_{jk\ell}^2/\alpha_{kj}^2\right)+1} = \frac{\phi_{k\ell}\beta_{\ell k\ell}^2/\alpha_{k\ell}^2}{\sum_{\substack{j=1\\ j\neq\ell}}^{L}\phi_{kj}\beta_{jk\ell}^2/\alpha_{kj}^2}. \tag{10}$$

Note that this limit depends mainly on the long-term fading coefficients β_{jki}, which are related to the spatial distribution of the users in the different cells.

3.2. Asymptotic limits of ZF beamforming

For the ZF beamforming, Eq. (8) becomes

$$r_{k\ell} = \sum_{l=1}^{L}\sum_{j=1}^{K}\sqrt{\phi_{jl}\beta_{lk\ell}}\,\mathbf{h}_{lk\ell}^H\mathbf{p}_{jl}^{zf}x_{jl} + n_{k\ell}. \tag{11}$$

In order to find the asymptotic limits when employing the ZF scheme, we begin analysing the matrix $\mathbf{A}_\ell = \left[\widehat{\mathbf{G}}_\ell\widehat{\mathbf{G}}_\ell^H\right]^{-1}$. From (3), we have that

$$\mathbf{A}_\ell = \left[\left(\sum_{j=1}^{L}\sqrt{\boldsymbol{\Gamma}_j\mathcal{B}_{\ell j}}\mathbf{H}_{\ell j} + \mathbf{N}'\right)\left(\sum_{l=1}^{L}\mathbf{H}_{\ell l}^H\sqrt{\boldsymbol{\Gamma}_l\mathcal{B}_{\ell l}} + \mathbf{N}'^H\right)\right]^{-1} \tag{12}$$

Note that from Lemma 1, we can neglect all the terms corresponding to products of independent matrices, since in the limit of $N\to\infty$, they will not account. So, (12) simplifies to:

$$\begin{aligned}\mathbf{A}_\ell &= \left[\sum_{j=1}^{L}\sqrt{\boldsymbol{\Gamma}_j\mathcal{B}_{\ell j}}\mathbf{H}_{\ell j}\sum_{l=1}^{L}\mathbf{H}_{\ell l}^H\sqrt{\boldsymbol{\Gamma}_l\mathcal{B}_{\ell l}} + \mathbf{N}'\mathbf{N}'^H\right]^{-1}\\ &= \left[\sum_{j=1}^{L}\sqrt{\boldsymbol{\Gamma}_j\mathcal{B}_{\ell j}}\mathbf{H}_{\ell j}\mathbf{H}_{\ell j}^H\sqrt{\boldsymbol{\Gamma}_j\mathcal{B}_{\ell j}} + \mathbf{N}'\mathbf{N}'^H\right]^{-1}\\ &= \left[N\left(\sum_{j=1}^{L}\boldsymbol{\Gamma}_j\mathcal{B}_{\ell j} + \frac{1}{K}\mathbf{I}_K\right)\right]^{-1}\\ &= [\mathbf{D}_\ell]^{-1}.\end{aligned} \tag{13}$$

It can be seen that the matrix $\mathbf{D}_\ell$ is a diagonal matrix, in which the kth term can be written as $[\mathbf{D}_\ell]_{kk} = N\left(\sum_{j=1}^{L}\gamma_{kj}\beta_{\ell kj} + \frac{1}{K}\right)$. Thus, the matrix $\mathbf{A}_\ell$ will also be a diagonal matrix, and the kth term can be written as $[\mathbf{A}_\ell]_{kk} = 1/[\mathbf{D}_\ell]_{kk}$. Hence, the vector $\mathbf{w}_{jk} = \widehat{\mathbf{G}}_j^H\mathbf{a}_{jk}$ is simplified to $\mathbf{w}_{jk} = \widehat{\mathbf{g}}_{jk}^H\frac{1}{N\left(\sum_{j=1}^{L}\gamma_{kj}\beta_{\ell kj}+\frac{1}{K}\right)}$, and Eq. (6) can be rewritten as

$$\mathbf{p}_{kj}^{zf} = \frac{\widehat{\mathbf{g}}_{jk}^H\frac{1}{N\left(\sum_{j=1}^{L}\gamma_{kj}\beta_{\ell kj}+\frac{1}{K}\right)}}{\left\|\widehat{\mathbf{g}}_{jk}^H\frac{1}{N\left(\sum_{j=1}^{L}\gamma_{kj}\beta_{\ell kj}+\frac{1}{K}\right)}\right\|} = \frac{\widehat{\mathbf{g}}_{jk}^H}{\left\|\widehat{\mathbf{g}}_{jk}^H\right\|} = \mathbf{p}_{kj}^{mf}. \tag{14}$$

It is important to note that the convergence of the MF precoding to the ZF scheme in the limit of $N\to\infty$ is just achieved when considering the constraint of maximum transmit power available at BS, *i.e.*, normalizing the precoding vector. Otherwise, the asymptotic performances of such techniques will differ, as shown in [14, Fig. 11]. Furthermore, this equality holds only for N very large. For intermediate values, it is seen that the ZF scheme approaches the asymptotic limit faster than the MF beamforming, as numerically demonstrated in Section 5.1. However, the MF technique is quite less complex, and can be implemented in a decentralized way since the precoding vector of each user is not dependent on the estimated channels of other users, as opposed to ZF.

3.3. Asymptotic BER in downlink

We demonstrated that the MF and ZF schemes converge to the same precoding vector when the number of BS antennas grows to infinity. So, the results obtained in [5] for MF are also valid for ZF, specially Eqs. (9) and (10). Analysing the received signal of the kth user of the ℓth cell (9), we can also obtain some information about the bit-error probability:

$$r_{k\ell} = \sqrt{N\gamma_{k\ell}}\left(\frac{\sqrt{\phi_{k\ell}}\beta_{\ell k\ell}x_{k\ell}}{\alpha_{k\ell}} + \sum_{\substack{l=1\\ l\neq\ell}}^{L}\frac{\sqrt{\phi_{kl}}\beta_{lk\ell}x_{kl}}{\alpha_{kl}}\right) + n_{k\ell}. \tag{15}$$

Indeed, the effect of AWGN is averaged out when $N\to\infty$. For notation simplicity, but with no loss of generality, we consider 4-QAM modulation. Thus, the probability of error for this user can be written as (16a) in the next page, where $\Pr(\cdot)$ is the probability of an event. Hence, (16a) can be simplified as (16b), since both terms in the sum have the same statistical behaviour. The errors will occur whenever the interfering signal that reaches the user is greater than its intended signal.

$$\begin{aligned}\mathrm{Pe}_{k\ell} &= \frac{1}{2}\Pr\left(\Re\left\{\frac{\sqrt{\phi_{k\ell}}\beta_{\ell k\ell}x_{k\ell}}{\alpha_{k\ell}}\right\} < \Re\left\{\sum_{\substack{l=1\\ l\neq\ell}}^{L}\frac{\sqrt{\phi_{kl}}\beta_{lk\ell}x_{kl}}{\alpha_{kl}}\right\}\right)\\ &\quad+\frac{1}{2}\Pr\left(\Im\left\{\frac{\sqrt{\phi_{k\ell}}\beta_{\ell k\ell}x_{k\ell}}{\alpha_{k\ell}}\right\} < \Im\left\{\sum_{\substack{l=1\\ l\neq\ell}}^{L}\frac{\sqrt{\phi_{kl}}\beta_{lk\ell}x_{kl}}{\alpha_{kl}}\right\}\right),\end{aligned} \tag{16a}$$

$$\begin{aligned}&= \frac{1}{2}\Pr\left(\frac{\sqrt{\phi_{k\ell}}\beta_{\ell k\ell}\Re\{x_{k\ell}\}}{\alpha_{k\ell}} < \sum_{\substack{l=1\\ l\neq\ell}}^{L}\frac{\sqrt{\phi_{kl}}\beta_{lk\ell}\Re\{x_{kl}\}}{\alpha_{kl}}\right)\\ &\quad+\frac{1}{2}\Pr\left(\frac{\sqrt{\phi_{k\ell}}\beta_{\ell k\ell}\Im\{x_{k\ell}\}}{\alpha_{k\ell}} < \sum_{\substack{l=1\\ l\neq\ell}}^{L}\frac{\sqrt{\phi_{kl}}\beta_{lk\ell}\Im\{x_{kl}\}}{\alpha_{kl}}\right),\\ &= \Pr\left(\frac{\sqrt{\phi_{k\ell}}\beta_{\ell k\ell}\Re\{x_{k\ell}\}}{\alpha_{k\ell}} < \sum_{\substack{l=1\\ l\neq\ell}}^{L}\frac{\sqrt{\phi_{kl}}\beta_{lk\ell}\Re\{x_{kl}\}}{\alpha_{kl}}\right).\end{aligned} \tag{16b}$$

In order to determine the exact value of the probability in (16b), we must analyse every possible combination of interfering signals. Thus, the result can be written as

$$\mathrm{Pe}_{k\ell} = \frac{1}{2^{L-1}}\sum_{j=1}^{2^{L-1}}\mathrm{u}\left[\left(\sum_{\substack{l=1\\ l\neq\ell}}^{L}\frac{\sqrt{\phi_{kl}}\beta_{lk\ell}b_{jl}}{\alpha_{kl}}\right) - \frac{\sqrt{\phi_{k\ell}}\beta_{\ell k\ell}}{\alpha_{k\ell}}\right] \tag{17}$$

where b_{jl} is the j,lth element of the $2^{L-1}\times L$ matrix $\mathbf{B} = [\mathbf{B}'_{1:\ell-1}, \mathbf{1}_{2^{L-1}}, \mathbf{B}'_{\ell:L-1}]$, in which $\mathbf{B}'$ contains every possible combination of $\{\pm1\}^{L-1}$. Although we restricted our investigation for 4-QAM modulation, similar analysis can be conducted for $M>4$ by appropriately defining the decision bounds for $r_{k\ell}$ in (15).

The expression in (17) gives the exact BER of the kth user of the ℓth cell, as a function of the powers and the long-term fading coefficients of users in adjacent cells sharing the same training sequence. Thus it can be adopted as a performance optimization metric, in the same way as defined in Eq. (10). One possible approach is invoking a power allocation algorithm, as done in [5] with respect to (10). In this paper, we prefer a more simple strategy, that consists of simply *optimizing the assignment of pilot sequences to users*, by knowing the interference experienced by each sequence. We call this procedure of pilot allocation scheme.

4. Pilot allocation schemes

Eq. (15) shows that the received signal for a given user in the downlink of a massive MIMO system presents interference from another users in adjacent cells that share the same pilot sequence.

Please cite this article in press as: Marinello JC, Abrão T. Pilot distribution optimization in multi-cellular large scale MIMO systems. Int J Electron Commun (AEÜ) (2016), http://dx.doi.org/10.1016/j.aeue.2016.05.007

Besides, from this received signal in the limit of $N \to \infty$, the asymptotic expressions for SINR, Eq. (10), and for BER, Eq. (17), have been derived. At first glance, it may appear that the interference term in (15) does not depend on which user in ℓth cell is assigned the kth pilot sequence. However, reminding that $\alpha_{kl}^2 \overset{a.s.}{=} \sum_{j=1}^{L} \gamma_{kj}\beta_{lkj} + \frac{1}{K}$, one can see it is not true.

Thus, varying to which user is assigned the kth pilot sequence according its long-term fading coefficient can enhance the SINR, Eq. (10), and/or[1] decrease the probability of error, Eq. (17). This fact allows us the formulation of alternative optimization criteria, as described in the sequel.

Initially, we define the matrix $\mathbf{C}$, of size $K! \times K$, containing every possible combination of pilot sequences to the users, *i.e.*, c_{ij} says that, in the ith combination, the jth pilot sequence is allocated to the c_{ij}th user. Then we define four pilot allocation criterion aiming to optimise BER or SINR figure of metric. The four criteria are described in the following.

4.1. MinBER-based pilot allocation metric

In the first pilot allocation scheme, we search the best pilot distribution in the sense of minimizing the mean BER among users of the ℓth cell, leading to the MinBER pilot allocation scheme:

$$i_{mb} = \arg \min_{i} \frac{1}{K} \sum_{k=1}^{K} \mathrm{Pe}_{c_{ik}\ell}, \tag{18}$$

in which

$$\mathrm{Pe}_{c_{ik}\ell} = \frac{1}{2^{L-1}} \times \sum_{j=1}^{2^{L-1}} \mathrm{u}\left[\left(\sum_{\substack{l=1 \\ l\neq\ell}}^{L} \frac{\sqrt{\phi_{kl}}\beta_{lk\ell} b_{jl}}{\alpha_{kl}^{(i)}} \right) - \frac{\sqrt{\phi_{c_{ik}\ell}}\beta_{\ell c_{ik}\ell}}{\alpha_{c_{ik}\ell}^{(i)}} \right]$$

corresponds to the BER of the c_{ik}th user of ℓth cell when the kth pilot sequence is assigned to him. Note that the superscript in $\alpha_{kl}^{(i)}$ and $\alpha_{c_{ik}\ell}^{(i)}$ evidences that these terms depend on the ith pilot distribution, since $\left(\alpha_{kl}^{(i)}\right)^2 = \gamma_{c_{ik}\ell}\beta_{lc_{ik}\ell} + \sum_{\substack{j=1 \\ j\neq\ell}}^{L} \gamma_{kj}\beta_{lkj} + \frac{1}{K}$, and $\left(\alpha_{c_{ik}\ell}^{(i)}\right)^2 = \gamma_{c_{ik}\ell}\beta_{\ell c_{ik}\ell} + \sum_{\substack{j=1 \\ j\neq\ell}}^{L} \gamma_{kj}\beta_{\ell kj} + \frac{1}{K}$, where we have put in evidence the terms related to the c_{ik}th user of the ℓth cell. The pilot allocation procedure is evaluated in a decentralized way; therefore, the assignment of pilots can be modified only for users of the ℓth cell when it is carrying out this procedure. Although the strictly optimal solution would test every possible pilot combination among the $K \cdot L$ users, its complexity would be prohibitive. Thus, the solution obtained in the decentralized way is preferable, and it can be shown that it converges to a Nash equilibrium after performing some times by each cell. Note that this problem can be viewed as a *finite potential game*, since: (a) it exists a global potential function that maps every strategy to some real value according its efficiency; (b) the set of strategies is of finite dimension [12]. In this case, each cell is a player, the potential function would be the average BER of the whole system in that subcarrier, *i.e.*, the average of (17) evaluated for the $K \cdot L$ users, and the strategy is the pilot allocation in that cell. Since each player chooses its strategy following a selfish best response dynamics, the convergence of the game to a Nash equilibrium is assured in [12, Theorem 19.12], [15, Proposition 2.2]. Besides, the decentralized solution can achieve appreciable gains in performance, as demonstrated in the next Section.

[1] Maximizing the SINR not necessarily minimizes the BER in the limit of $N \to \infty$, as can be seen from expressions (10) and (17), and discussed in Section 5.2.

4.2. MaxSINR-based pilot allocation metric

In the same way, in the second pilot allocation scheme, we define the pilot distribution that maximizes the mean SINR in the downlink of the ℓth cell, namely MaxSINR pilot allocation scheme:

$$i_{\mathrm{ms}} = \arg \max_{i} \frac{1}{K} \sum_{k=1}^{K} \mathrm{SINR}_{c_{ik}\ell}^{\mathrm{dl}}, \tag{19}$$

in which

$$\mathrm{SINR}_{c_{ik}\ell}^{\mathrm{dl}} = \frac{\phi_{c_{ik}\ell}\beta_{\ell c_{ik}\ell}^2 / \left(\alpha_{c_{ik}\ell}^{(i)}\right)^2}{\sum_{\substack{j=1 \\ j\neq\ell}}^{L} \phi_{kj}\beta_{jk\ell}^2 / \left(\alpha_{kj}^{(i)}\right)^2} \tag{20}$$

is the downlink SINR of the c_{ik}th user of ℓth cell when the kth pilot sequence is assigned to him.

4.3. MiniMaxBER-based pilot allocation metric

Both optimization schemes, *e.g.* (18) and (20), find the pilot distribution by optimizing the mean value of some performance criterion. However, the "average" approach may be not completely adequate in modern communications systems, since it may lead to a great improvement in performance for a few users, while providing low quality of service (QoS) to those users poorly located, typically in the edge of the cell. Hence, we also look for pilot allocation schemes that ensure improvement in QoS for every user within the ℓth cell. The MinimaxBER pilot allocation scheme is defined as:

$$i_{mmb} = \arg \min_{i} \max_{k} \mathrm{Pe}_{c_{ik}\ell}, \tag{21}$$

which minimizes the worst BER within the cell.

4.4. MaxMinSINR-based pilot allocation metric

On the other hand, the MaxminSINR pilot allocation criterion constitutes an alternative way to optimally allocate pilots in multi-celular massive MIMO systems. The MaxminSINR pilot allocation scheme can be defined from the following optimization problem:

$$i_{mms} = \arg \max_{i} \min_{k} \mathrm{SINR}_{c_{ik}\ell}^{dl}, \tag{22}$$

which finds the pilots' set that maximizes the lowest SINR among the users of the cell.

4.5. Pilot allocation algorithm and its complexity

In the analysis of the pilot allocation strategies for multi-cellular massive MIMO we have assumed the asymptotic condition, i.e, when $N \to \infty$. Hence, the complexity of implementation of these pilot allocation algorithms will be independent of the number of antennas N. Algorithm 1 describes the general pilot allocation procedure, defining its inputs, outputs, and main steps. After its computation, the ℓth cell assigns the kth pilot sequence to the $c_{i_{opt}k}$th user. Note that each cell should be able to find the optimal pilot combination set among its covered users following one of these four criteria given respectively by Eq. (18), (19), (21), (22), in a decentralized way, reducing the overall computational complexity of the massive MIMO system.

Indeed, the computational complexity for the SINR-based pilot allocation procedures results $\mathcal{O}(K! \cdot K \cdot L^2)$, since operation of lines 4 and 6 demands $2L + 1$ *flops* (floating point operations) each one, and will be evaluated $K! \cdot K \cdot L$ times. On the other hand, the

Please cite this article in press as: Marinello JC, Abrão T. Pilot distribution optimization in multi-cellular large scale MIMO systems. Int J Electron Commun (AEÜ) (2016), http://dx.doi.org/10.1016/j.aeue.2016.05.007

BER-based pilot allocation schemes result in a computational complexity of $\mathcal{O}(K! \cdot K \cdot L \cdot 2^{L-1})$, since evaluation of Eq. (18) or (21) in line 10 becomes prevalent, *i.e.* of $\mathcal{O}(K \cdot L \cdot 2^{L-1})$, and should be evaluated for the $K!$ pilot combinations. Such complexities may appear excessive. However, bearing in mind that K must assume low values in practical scenarios,[2] as well as the number L of cells within a cluster, one can conclude that the complexity of pilot allocation procedures is not prohibitive. As described in [9], there is no appeal to consider higher values of K in practical mobile TDD massive MIMO scenarios, since great part of the coherence time interval would be spent acquiring CSI from the moving terminals. Besides, once the optimization is complete, it remains valid for a relatively large time-interval, since the scheme depends only on the transmit powers and long-term fading coefficients of the users. Even for specific scenarios in which K may assume higher values, *i.e.*, with reduced mobility such as pedestrian scenarios, the exhaustive search approach can be replaced by some low-complexity heuristic method, and the optimization remains valid.

Algorithm 1 Pilot allocation procedure

Input: $\mathcal{B}_{jl}, \mathbf{\Phi}_j, \mathbf{\Gamma}_j, \forall j, l = 1, 2, \ldots L$.

1: Generate matrix $\mathbf{C}$, of size $K! \times K$;
2: **for** each combination $i = 1, 2, \ldots, K!$ **do**
3: **for** each pilot sequence $k = 1, 2, \ldots, K$ **do**
4: Evaluate $\alpha_{c_{ik}\ell}^{(i)} = \sqrt{\gamma_{c_{ik}\ell}\beta_{\ell c_{ik}\ell} + \sum_{\substack{j=1 \\ j\neq\ell}}^{L}\gamma_{kj}\beta_{\ell kj} + \frac{1}{K}}$;
5: **for** each cell $l = 1, 2, \ldots, L, l \neq \ell$ **do**
6: Evaluate $\alpha_{kl}^{(i)} = \sqrt{\gamma_{c_{ik}\ell}\beta_{lc_{ik}\ell} + \sum_{\substack{j=1 \\ j\neq\ell}}^{L}\gamma_{kj}\beta_{lkj} + \frac{1}{K}}$;
7: **end for**
8: **end for**
9: **end for**
10: Find $i_{opt} \in i = 1, 2, \ldots, K!$, corresponding to the optimal combination in $\mathbf{C}$ according some metric: (18), (19), (21), (22);
Output: i_{opt}.

5. Numerical results

Aiming to demonstrate the effectiveness of the proposed pilot allocation methods for multi-cellular massive MIMO systems, we provide in this Section performance results for both BER and SINR downlink metrics. The asymptotic condition ($N \to \infty$) for the number of BS antennas has been assumed, except for the convergence analysis for increasing N depicted in Fig. 2. We have adopted a multi-cell scenario with hexagonal cells of radius 1600 m, where $K = 4$ users are uniformly distributed in its interior, except in a circle of 100m radius around the cell centered BS. Besides, only the first ring of interfering cells has been considered, both for frequency reuse factors (RF) of one and three. We have assumed a similar TDD protocol of that in [5], in which the coherence interval is composed of 11 symbol periods: 4 for sending uplink training sequences, 1 for processing, 4 and 2 for downlink and uplink data transmission, respectively. As discussed in [8], in order to maximize the net throughput for a TDD protocol, it is beneficial to dedicate the same time with pilots and data transmissions. If more time is spent with pilots, more users can be served, but its rates decrease substantially due to the excessive overhead, and vice-versa. The system uses a carrier frequency of 1.9 GHz and a frequency band of 20 MHz.

Furthermore, the coherence time of 500 microseconds has been adopted, which could accommodate any terminal moving slower than 80 meters/second (associating the coherence time with the interval required by a terminal to move no more than 1/4 wavelength [9, Sec.VII-D]). The log-normal shadowing has been modelled with a standard deviation of 8dB, and the path loss term $d_{\ell kj}^{-\lambda}$ with decay exponent equal to $\lambda = 3.8$, and $d_{\ell kj}$ denoting the distance between the ℓth BS to kth mobile user of jth cell. Besides, we have considered 4-QAM modulation, a SNR target of 10 dB and an equal power allocation policy for all users, valid both for downlink[3] and uplink. The constraint of maximum transmit power available at BS is satisfied by the precoding schemes in our formulation, as represented in expressions (5) and (6), in which the precoding vectors are normalized. It is important to note that the numerical results in this Section (except part of Fig. 2) were obtained from the analytical expressions derived in Section 3, averaged from the evaluation of at least 10^5 independent trials for the user's location.

Fig. 1 depicts a single realization of the multi-cell scenario adopted in our numerical simulations, for frequency reuse factors of one and three. Notice that for clarity purpose, only users sharing the same frequency band, *i.e.*, interfering with each other, have been represented. Indeed, one can see that interfering users are much closer with smaller reuse factors. In our numerical results presented in the sequel, only the performance metrics of users positioned inside the central cell were computed, since these users experience a more realistic condition of interference.

5.1. Performance convergence of precoding techniques

Considering both MF and ZF precoding techniques, Fig. 2 depicts the asymptotic convergence[4] (as the number of BS antennas increases) for both BER and SINR performance metrics to the bounds defined in (17) and (10), respectively. The curves present mean values of each performance metric, taken among the users of the cell. One can note that the SINR of the ZF precoding scheme indeed converges to the same bound of Eq. (10), which was derived in [5] as the asymptotic SINR of MF beamforming. This occurs since we have considered the constraint of maximum transmit power available at BS, as opposed to [14]. These numerical results also show that MF needs at least one order of magnitude more BS antennas than ZF to reach that bound. Furthermore, the performance of both schemes are also analysed from the perspective of BER, validating Eq. (17) as the asymptotic BER that such techniques are able to achieve when $N \to \infty$. Indeed, in terms of BER, the performances of both techniques rapidly approach the asymptotic limit, being necessary $\approx 10^4$ BS antennas for both precoding techniques reaching the bound.

5.2. Performance of pilot allocation schemes

In this subsection, we investigate the performance of the four pilot allocation schemes proposed in Section 4, in terms of mean values, as well as in terms of distribution among users. The simu-

[2] K represents the length of the training sequences, which is equal to the number of users sharing one of N_{smooth} subcarriers in each coherence band. N_{smooth}, as given in (1), is desired to be high for an efficient OFDM communication; for example, $N_{\text{smooth}} = 14$ for $\Delta t_{CP} = 7\%$. On the other hand, K is limited by the coherence time, due to the user's mobility, by the efficiency of the TDD scheme, which cannot spend much time with pilots, and by the subcarrier spacing. For example, in [9], for a cell serving 42 users, $K = 3$ and $N_{\text{smooth}} = 14$.

[3] Despite of the average equal power allocation policy, the instantaneous power for users in downlink may differ due to the precoding scheme.

[4] Notice that in Fig. 2 simulation and analysis results have been compared, since performances of the techniques for increasing N are computed with independent realizations of small-scale fading, AWGN, and long-term fading, and they converge to the analytical bounds dependent only on the long-term fading.

Please cite this article in press as: Marinello JC, Abrão T. Pilot distribution optimization in multi-cellular large scale MIMO systems. Int J Electron Commun (AEÜ) (2016), http://dx.doi.org/10.1016/j.aeue.2016.05.007

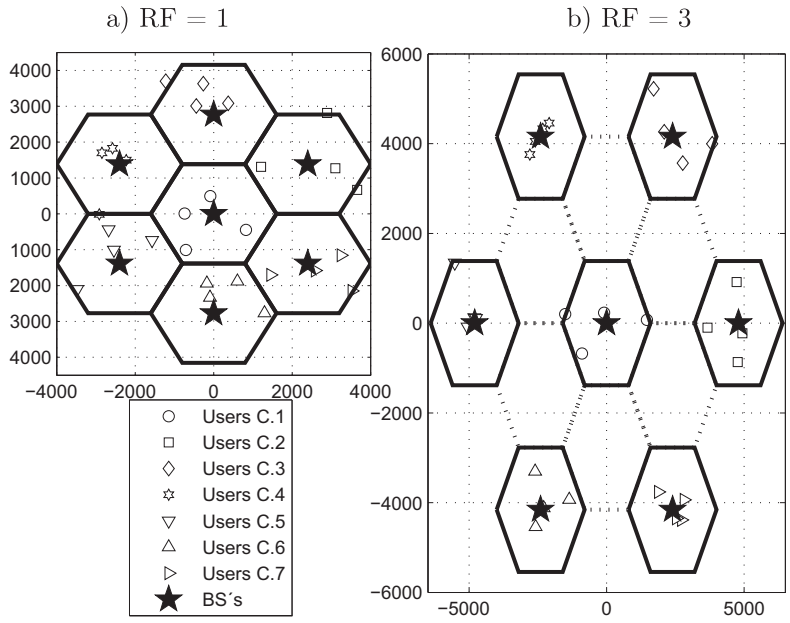

Fig. 1. Single spatial realization for both investigated multi-cell scenarios, with $K = 4$ mobile terminals.

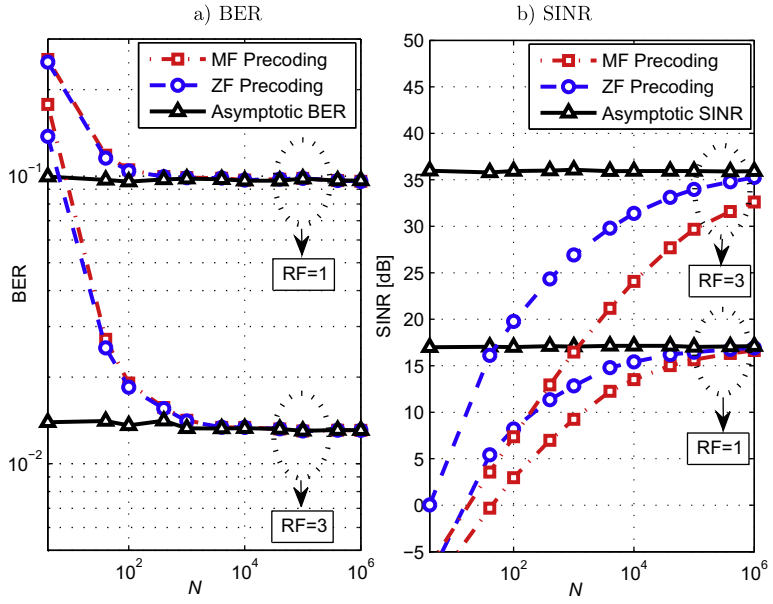

Fig. 2. Asymptotic convergences of MF and ZF precoding techniques to the performance bounds, under reuse factors of one and three, with increasing N.

lation results presented here were averaged over 100,000 spatial realizations.

Fig. 3 shows the cumulative distribution function (CDF) as a function of the BER of the users, regarding different pilot allocation techniques. For reference of comparison, it is also depicted the very large MIMO performance with no optimization in the distribution of pilot sequences, *i.e.*, with random allocation strategy. An interesting behavior on the BER distribution among users in the massive MIMO system can be observed from these numerical results. One can note that a significant portion of users communicates to BS with no errors, *i.e.*, BER = 0. This occurs because, for these users, even the strongest interference that can reach them is lower than their intended signal, and thus the probability of error is null. On the other hand, the other small portion of users, that are not free of errors, presents excessive values of BER. This disparity becomes more noticeable for unitary frequency reuse factor, in which the portion of users that presents excessive error rates is $\approx 10\%$, while for reuse factor of three it is about 1% for a BER $\geqslant 0.2$.

Furthermore, it shows that the pilot allocation schemes are able to significantly decrease the fraction of users with excessive BER's. As shown in Tables 1 and 2, the fraction of users with BER $\geqslant 0.1$ reduces from 23.63% to 14.92%, for frequency reuse factor of one, and from 3.47% to 1.06%, for frequency reuse factor of three, when deploying the MinBER approach.

Fig. 4 shows the fraction of users above a given SINR, for frequency reuse factors of one and three. It can be seen that increasing the frequency reuse factor has the effect of significantly improving the SINR of the users, as if the curve was shifted right

Please cite this article in press as: Marinello JC, Abrão T. Pilot distribution optimization in multi-cellular large scale MIMO systems. Int J Electron Commun (AEÜ) (2016), http://dx.doi.org/10.1016/j.aeue.2016.05.007

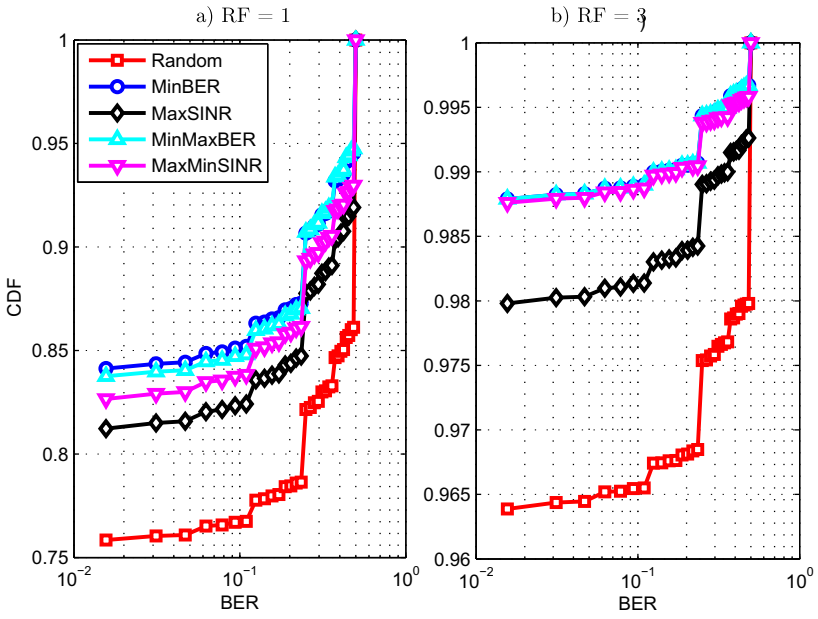

Fig. 3. Cumulative distribution function for the BER of the users, for different pilot allocation schemes.

Table 1
Performance of pilot allocation schemes for frequency-reuse factor of one.

PA scheme	Mean BER (%)	Users BER = 0 (%)	Users BER ⩾ 0.1 (%)	Mean user rate (Mbps)	95%-likely user rate (Mbps)
Random	9.84	75.41	23.63	48.50	0.1344
MinBER	5.48	83.98	14.92	55.54	0.4471
MaxSINR	6.85	80.85	17.78	56.59	0.4611
MinimaxBER	5.52	83.68	15.21	55.48	0.4609
MaxminSINR	6.17	82.45	16.28	52.62	0.7937

Table 2
Performance of pilot allocation Schemes for frequency-reuse factor of three.

PA scheme	Mean BER (%)	Users BER = 0 (%)	Users BER ⩾ 0.1 (%)	Mean user rate (Mbps)	95%-likely user rate (Mbps)
Random	1.41	96.33	3.47	29.07	4.79
MinBER	0.36	98.83	1.06	32.84	8.82
MaxSINR	0.66	98.01	1.86	32.91	8.81
MinimaxBER	0.37	98.82	1.06	32.84	8.82
MaxminSINR	0.39	98.78	1.09	31.68	11.15

$\approx$ 18 dB, without noticeable changes on its format and slope. One can see that the MaxSINR technique has the ability of improving the SINR of the best located users, increasing $\approx$ 4 dB of SINR for the best 20% of the users. On the other hand, the MaxminSINR scheme increases $\approx$ 10 dB of SINR for the 95% level, *i.e.*, it benefits the less favorably located users.

Finally, Fig. 5 depicts the fraction of users above a given data rate, for frequency reuse factors of one and three, regarding the different proposed pilot allocation schemes. Notice that the downlink data rate $\mathcal{R}_{k\ell}$ of the kth user in the ℓth cell can be defined as:

$$\mathcal{R}_{k\ell} = \left(\frac{bw}{rf}\right)\left(\frac{\mathcal{D}}{\mathcal{T}}\right)\log_2\left(1+\text{SINR}_{k\ell}^{dl}\right), \tag{23}$$

where bw is the system total bandwidth, rf is the reuse factor, $\mathcal{D}$ is the number of symbol periods spent sending downlink data, and $\mathcal{T}$ is the total number of symbol periods within a channel coherence time.

Examining the curves, one can conclude that the slope of curves for reuse factor three is greater than the slope of unitary reuse factor curves. This fact means that the distribution for unitary reuse factor is much more irregular, unequal, in the sense that some users have very high rates while others have low QoS. On the other hand, for reuse factor of three, this distribution is much more uniform, guaranteeing simultaneously an improved QoS for much more users.

As shown in Table 1, 95% of users communicates with rates greater than 0.1344 Mbps with random pilot distribution, while when employing the MaxminSINR PA scheme the 95%-likely rate per user increases to 0.7937 Mbps. This means that a gain of 6 times can be achieved for unitary frequency reuse factor, while providing a mean rate of 52.62 Mbps per user. Furthermore, if the minimum assured performance per terminal is a more important concern, then the MaxminSINR scheme can be employed in conjunction with a frequency reuse factor of three. As described in Table 2, the 95%-likely rate passes from 4.79 Mbps to 11.15 Mbps, a gain greater than 6 Mbps. Note that the mean rate, however, decreases, since the gain in SINR for the best located users does not offset the loss due to reduction in bandwidth, given the logarithmic increase of rate according SINR gains. Larger reuse

Please cite this article in press as: Marinello JC, Abrão T. Pilot distribution optimization in multi-cellular large scale MIMO systems. Int J Electron Commun (AEÜ) (2016), http://dx.doi.org/10.1016/j.aeue.2016.05.007

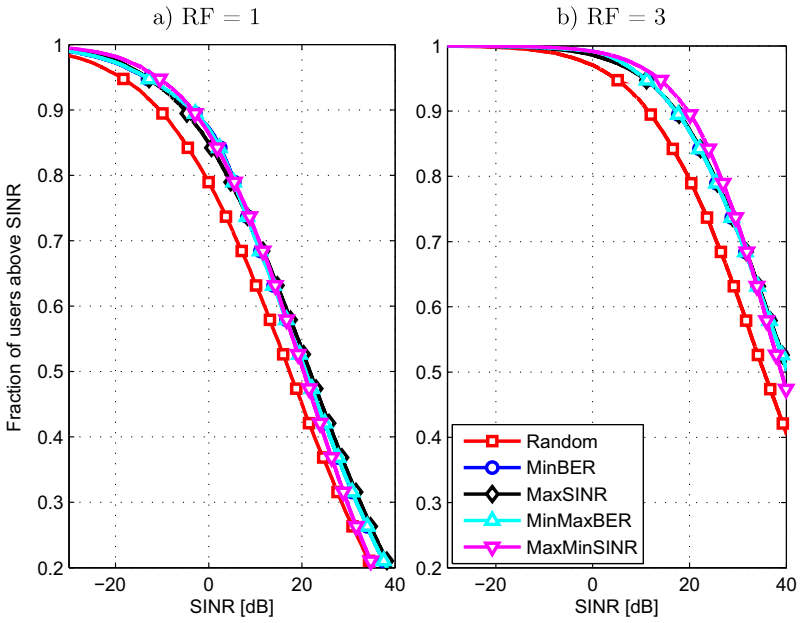

Fig. 4. Fraction of users above a given SINR, for different pilot allocation schemes.

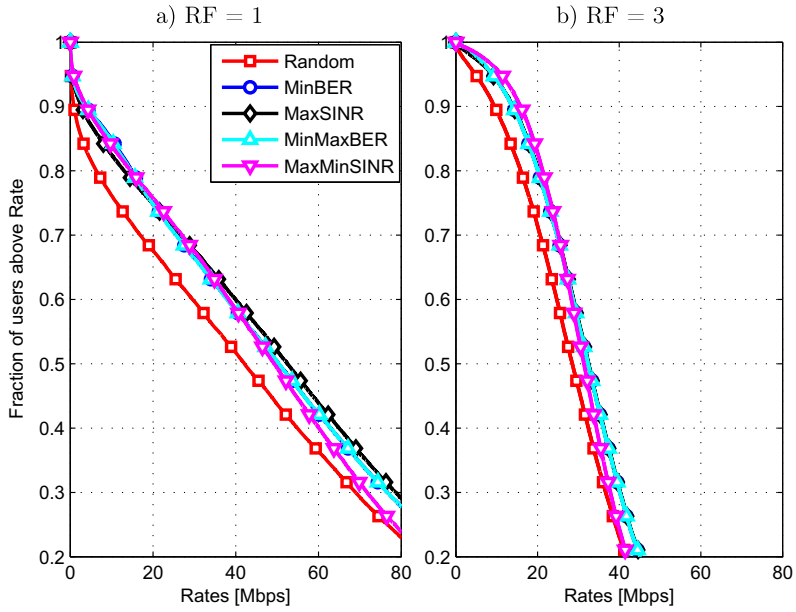

Fig. 5. Fraction of users above a given Rate, for different pilot allocation schemes.

factors are more beneficial for poor located users, since the logarithm is in its linear region, as discussed in [9].

Comparing both Tables, we note that the assured QoS, in terms of 95%-likely rate, can pass from 0.1344 Mbps, with unitary reuse factor and random pilot allocation, to 11.15 Mbps, for the Maxmin-SINR scheme and reuse factor of three. Thus, gains of ≈85 times can be achieved combining both RF and PA techniques, with appropriate conditions. Besides, the mean BER reduces from 9.84% to 0.39%, and the portion of users communicating in the absence of errors increases from 75.41% to 98.78%. These benefits are achieved by simply assigning the pilot sequences to the users within the cell in a more efficient way, in conjunction with a large frequency reuse factor, and remain valid whenever the long-term fading coefficients stay unchanged.

6. Conclusion

In this work we have characterized the asymptotic performance of the massive MIMO system downlink under the point of view of the BER performance. We have demonstrated that both MF and ZF precoding schemes result in the same signal as $N \to \infty$, and thus the results of [5] are also valid for the ZF beamforming. Then, we derived the exact asymptotic expression of the BER of a given user, based on the long-term fading coefficients and the power levels of other users. In the same way as the asymptotic SINR expression found in [5], the BER expression derived also depends only on the users in neighboring cells that reuse the same pilot sequence.

Furthermore, we have proposed efficient forms of assigning these pilots to the users within the cell, by optimizing several per-

Please cite this article in press as: Marinello JC, Abrão T. Pilot distribution optimization in multi-cellular large scale MIMO systems. Int J Electron Commun (AEÜ) (2016), http://dx.doi.org/10.1016/j.aeue.2016.05.007

formance metrics, including the asymptotic BER or alternatively the maximization of SINR found herein. The significant gains achieved by these pilot allocation techniques were demonstrated numerically. For instance, we have showed that a gain of 6 times regarding the random strategy can be achieved for the downlink rate with unitary reuse factor, while the data rate is increased from 4.79 Mbps to 11.15 Mbps for reuse factor of three. When combining the MaxminSINR technique with an appropriated reuse factor, we showed that the massive MIMO system are able to operate with a 95%-likely downlink rate of 11.15 Mbps, providing a communication free of errors for 98.78% of the users, guaranteeing the reliability of the system.

All of these benefits are achieved in a quite simple and expeditious way, by just knowing the powers and the long-term fading coefficients of users in adjacent cells, for each pilot sequence. Since these informations do not scale with the number of BS antennas, and remains constant within a long time and frequency interval, the implementation of the proposed pilot training sequence assignment method in massive MIMO system is surely feasible. Besides, even greater gains might be achieved by combining the proposed schemes with power allocation and time-shifting techniques [5,13], which is the continuity of this work.

Acknowledgement

This work was supported in part by the National Council for Scientific and Technological Development (CNPq) of Brazil under Grant 304066/2015-0, and in part by Londrina State University – Paraná State Government (UEL).

References

[1] Ashikhmin A, Marzetta T. Pilot contamination precoding in multi-cell large scale antenna systems. In: IEEE international symposium on information theory proceedings (ISIT), 2012. p. 1137–41.
[2] Boccardi F, Heath R, Lozano A, Marzetta T, Popovski P. Five disruptive technology directions for 5G. IEEE Commun Mag 2014;52(2):74–80.
[3] Choi J, Chance Z, Love D, Madhow U. Noncoherent trellis coded quantization: a practical limited feedback technique for massive MIMO systems. IEEE Trans Commun 2013;61(12):5016–29.
[4] Couillet R, Debbah M. Signal processing in large systems: a new paradigm. IEEE Signal Process Mag 2013;30(1):24–39.
[5] Fernandes F, Ashikhmin A, Marzetta T. Inter-cell interference in noncooperative TDD large scale antenna systems. IEEE J Sel Areas Commun 2013;31(2):192–201.
[6] Hanzo L, Akhtman Y, Wang L, Jiang M. MIMO-OFDM for LTE, WiFi and WiMAX: coherent versus non-coherent and cooperative turbo transceivers. IEEE Press and John Wiley & Sons; 2010.
[7] Karakayali M, Foschini G, Valenzuela R. Network coordination for spectrally efficient communications in cellular systems. IEEE Wirel Commun 2006;13(4):56–61.
[8] Marzetta T. How much training is required for multiuser MIMO? In: Fortieth asilomar conference on signals, systems and computers, ACSSC '06, 2006. p. 359–63.
[9] Marzetta T. Noncooperative cellular wireless with unlimited numbers of base station antennas. IEEE Trans Wireless Commun 2010;9(11):3590–600.
[10] Mazrouei-Sebdani M, Krzymien W, Melzer J. Massive MIMO with non-linear precoding: large-system analysis. IEEE Trans Veh Technol 2015;PP(99). 1–1.
[11] Ngo HQ, Larsson E, Marzetta T. Energy and spectral efficiency of very large multiuser MIMO systems. IEEE Trans Commun 2013;61(4):1436–49.
[12] Nisan N, Roughgarden T, Tardos E, Vazirani VV. Algorithmic game theory. Cambridge University Press; 2007.
[13] Rasti M, Sharafat A-R. Distributed uplink power control with soft removal for wireless networks. IEEE Trans Commun 2011;59(3):833–43.
[14] Rusek F, Persson D, Lau BK, Larsson E, Marzetta T, Edfors O, Tufvesson F. Scaling up MIMO: opportunities and challenges with very large arrays. IEEE Signal Process Mag 2013;30(1):40–60.
[15] Voorneveld M. Best-response potential games. Econ Lett 2000;66(3):289–95.
[16] Yang H, Marzetta T. Performance of conjugate and zero-forcing beamforming in large-scale antenna systems. IEEE J Sel Areas Commun 2013;31(2):172–9.
[17] Zheng K, Zhao L, Mei J, Shao B, Xiang W, Hanzo L. Survey of large-scale MIMO systems. IEEE Commun Surv Tutorials 2015;17(3):1738–60.
[18] Zhu X, Wang Z, Qian C, Dai L, Chen J, Chen S, Hanzo L. Soft pilot reuse and multi-cell block diagonalization precoding for massive MIMO systems. IEEE Trans Veh Technol 2015;PP(99). 1–1.

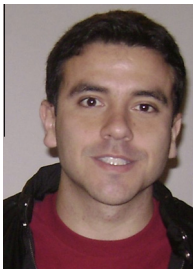

José Carlos Marinello received his B.S. and M.S. degree in Electrical Engineering (the first with Summa Cum Laude) from Londrina State University, PR, Brazil, in December 2012 and Sept 2014, respectively. He is currently working towards his Ph.D. at Polytechnic School of Sao Paulo University, São Paulo, Brazil. His research interests include physical layer aspects, such as heuristic and convex optimization of 4G and 5G MIMO systems.

Taufik Abrão (SM'12) received the B.S., M.Sc., and Ph.D. degrees in electrical engineering from the Polytechnic School of the University of São Paulo, São Paulo, Brazil, in 1992, 1996, and 2001, respectively. Since March 1997, he has been with the Communications Group, Department of Electrical Engineering, Londrina State University, Londrina, Brazil, where he is currently an Associate Professor of Communications engineering. In 2012, he was an Academic Visitor with the Communications, Signal Processing and Control Research Group, University of Southampton, Southampton, U.K. From 2007 to 2008, he was a Post-doctoral Researcher with the Department of Signal Theory and Communications, Polytechnic University of Catalonia (TSC/UPC), Barcelona, Spain. He has participated in several projects funded by government agencies and industrial companies. He is involved in editorial board activities of six journals in the communication area and he has served as TPC member in several symposium and conferences. He has been served as an Editor for the IEEE COMMUNICATIONS SURVEYS & TUTORIALS since 2013. He is a member of SBrT and a senior member of IEEE. His current research interests include communications and signal processing, specially the multi-user detection and estimation, MC-CDMA and MIMO systems, cooperative communication and relaying, resource allocation, as well as heuristic and convex optimization aspects of 3G and 4G wireless systems. He has co-authored of more than 170 research papers published in specialized/international journals and conferences.